Dynamics of the strain-mediated phase transition in $KDCO_3$: A thermal neutron spin-echo study

K. Kakurai, T. Sakaguchi, and M. Nishi
Neutron Scattering Laboratory, Institute of Solid State Physics, University of Tokyo, 106-1 Shirakata, Tokai, Ibaraki 319-11, Japan

C. M. E. Zeyen
Institut Laue Langevin, Boîte Postale 156, F-38042 Grenoble Cedex 9, France

S. Kashida
Faculty of Science, Niigata University, Ikarashi, Niigata 950-21, Japan

Y. Yamada
Advanced Research Center for Science and Engineering, Waseda University, Okubo, Shinjuku-ku, Tokyo 169, Japan
(Received 27 November 1995)

The dynamical aspects of the order-disorder phase transition in $KDCO_3$ are studied by means of thermal-neutron spin-echo triple-axis spectrometry with a high-energy resolution of ~ 0.2 μeV. Besides the critical slowing down of the correlated fluctuations of the $(DCO_3)_2$ dimers, temperature-dependent fluctuations of the strain field caused by the individual low-symmetry dimers are seen in the form of dynamical Huang scattering around the main Bragg peak. An interesting mechanism for the order-disorder phase transition, namely a strain-mediated phase transition, is examined from a dynamical point of view.

INTRODUCTION

The proton dynamics in potassium bicarbonate as well as in carboxylic acids have been attracting much attention because both quantum tunneling and vibrational excitations are expected to play important roles in the jump of protons forming the hydrogen bond. The nature of the proton dynamics in potassium bicarbonate has been studied using various methods such as IR and Raman spectroscopy,[1,2] NMR,[3] x-ray,[4] and inelastic neutron scattering.[5] Disorder of hydrogen is observed and attributed to concerted proton jumps.[4] Inelastic neutron-scattering results[5] and detailed analysis of IR data[6] indicate the coupling of the proton (or deuteron) transfer to a ''heavy atom mode'' which is suggested to be the rocking mode of the $(HCO_3)_2$ dimer around the c axis, as first proposed for carboxylic acids.[7]

On the other hand, it has been known that $KHCO_3$ crystal undergoes a structural phase transition where the low-temperature structure is characterized by the tilting of $(HCO_3)_2$ dimer. A sign of the structural phase transition in $KHCO_3$ was found by Haussühl[8] during ultrasonic velocity measurements at 318 K. The subsequent x-ray-diffraction study by Kashida and Yamamoto[9] revealed that indeed an order-disorder structural phase transition occurs at 318 K from the $C2/m$ high-temperature phase to the $P2_1/a$ low-temperature phase. The structure in the low-temperature phase is shown in Fig. 1(b). The long principal axes of the $(HCO_3)_2$ dimers are tilted in antiphase at the center and corner sites of a-b plane. The potassium atoms are also shifted in their positions alternately along the b axis.[9] In the high-temperature phase the dimers recover a higher symmetry as shown in Fig. 1(a).

An incoherent neutron-scattering experiment on $KHCO_3$ near the phase transition provided evidence that the proton transfer is strongly coupled to the fluctuations of the dimer orientations.[10] While no softening of any particular phonon branch has been observed, Eckhold *et al.*[10] report the existence of quasielastic diffusion scattering extending along the a^* axis. Recently Kanao *et al.*[11] studied neutron coherent scattering in $KDCO_3$. They investigated the detailed nature of the diffusion scattering above the transition temperature. The diffuse scattering observed around the superlattice point just above T_c can be characterized by the critical scattering associated with the correlated dimer fluctuation. In addition, it is found that there exists another type of diffuse scattering around the main Bragg peaks which persists well above T_c. From the very unique distribution around the Bragg peak positions (see inset of Fig. 1), this diffuse scattering is identified to be the strain field scattering (Huang scattering) caused by the individual deformed dimer which is locally breaking the symmetry of the lattice. The deformed dimer is properly characterized as the deuteron ''self-trapped state.''[11] The global high symmetry in the high-temperature phase is considered to be recovered by the temporal, as well as the spatial, average of the two degenerated proton ''self-trapped states'' of each dimer.

In contrast to the ordinary Huang scattering due to a static impurity, one expects some dynamics associated with the strain field scattering in the present case. Detailed investigation of the dynamical nature of the diffuse scatterings would clarify the coupling mechanisms between proton (deuteron) hopping motion and the lattice vibrational motion which plays a crucial role in the triggering of the phase transition.

In this paper we report the slow dynamics in the coherent diffuse scattering of $KDCO_3$ near the phase transition studied by means of the spin-echo option on the polarized neutron triple axis spectrometer which achieves a spectral resolution of a few tenths of μeV. Direct evidence for the inelastic nature of the above mentioned strain field scattering has been obtained. The temperature dependence of its inelasticity can

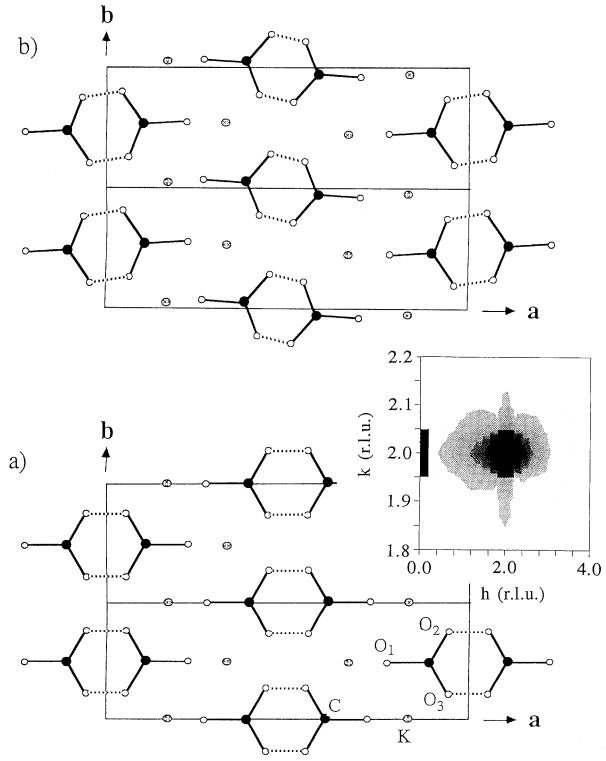

FIG. 1. Schematic drawing of $KHCO_3$ crystal structure projected on the a-b plane (a) in the high-temperature phase belonging to the space group $C2/m$ and (b) in the low-temperature phase belonging to the space group $P2\underline{1}/a$. The symmetry of $(HCO_3)_2$ dimer is lowered from $2mm$ to 1 upon transition. The hydrogen bonds are represented by dotted lines. Inset: The observed diffuse intensity distribution around (2,2,0) at $T=373$ K (from Ref. 11).

be directly related to the hopping motion between the two degenerate deuteron self-trapped states and viewed as direct evidence for the strain-mediated phase transition in $KDCO_3$.

SAMPLE AND INSTRUMENT

The single crystal was prepared from a concentrated solution of analytical grade $KDCO_3$. The colorless prismatic crystal of $\sim$1.5 cm^3 is oriented with its a^* and b^* axis in the scattering plane. The sample was mounted in a displex and the temperature was stabilized to within 0.1 K. To study the dynamics of the diffuse scattering neutron spin-echo spectroscopy was performed on the Institute of Solid State Physics, thermal polarized neutron triple axis (PONTA) spectrometer installed at the JRR-3M research reactor of the Japanese Atomic Energy Research Institute (JAERI) equipped with the normal-conducting optimal field shape (OFS) precession coils recently developed in collaboration with Institut Laue Langevin (Grenoble, France), Tohoku University (Sendai, Japan), and TOKIN Corp. (Sendai, Japan).[12] In the neutron spin-echo spectroscopy experiment both the incoming and outgoing velocity of a neutron are measured by making use of the Larmor precession of the neutron spin. The Larmor precessions over a well-defined field integral path serve as a ''spin clock'' attached to each individual neutron. It can be shown that the neutron spin-echo polarization corresponds to the ω Fourier transform of the scattering function $S(k,\omega)$ as

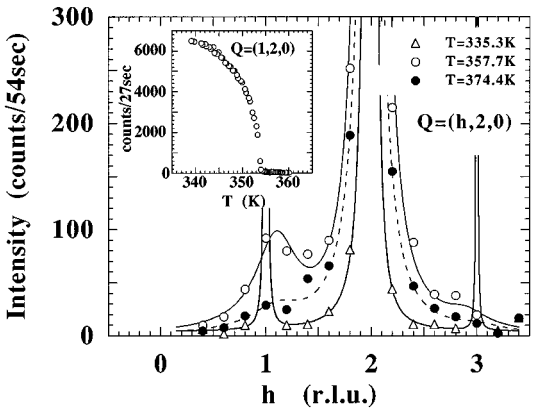

FIG. 2. Elastic scattering observed at $Q=(h,2,0)$ in normal triple axis mode with an energy window of $\sim$2 meV at various temperatures. The continuous and broken lines are guides for the eye. Inset: Temperature dependence of elastic scattering at the superlattice position (1,2,0) under the same experimental condition.

singled out by the resolution ellipsoid of the background triple axis spectrometer. (For the details of the spin-echo method see, e.g., Ref. 13.) For example, if $S(k,\omega)$ is given by a Lorentzian line in ω, whose linewidth Γ is narrow compared to the energy resolution of the background spectrometer, the Fourier time dependence of the spin-echo polarization is represented by an exponential decay with Γ as the relaxation coefficient. Thus, from the measurement of the spin-echo polarization for different Fourier times, i.e., with different precession field integrals, one can determine the linewidth Γ. The spin-echo option on a thermal neutron triple axis instrument makes it possible to reach a relative energy resolution of $\Delta E/E_i \sim 10^{-5}$, thus allowing us to perform high-energy-resolution experiments up to large Q($\sim$3.8 $Å^{-1}$) with a good Q resolution of $\Delta Q/Q \sim 10^{-2}$ which were mandatory for the results presented in this paper.

EXPERIMENTAL RESULTS

In the inset of Fig. 2 the temperature dependence of the peak intensity of the superlattice peak at $Q=(1,2,0)$ is depicted. The disappearance of the superlattice peak at around 354 K indicates the phase transition to the high-temperature $C2/m$ structure.

Figure 2 shows the elastic intensity distribution along $(h,2,0)$ at three different temperatures taken in the conventional triple axis mode with an energy window of $\sim$2 meV. At $T=335$ K, below T_c, sharp Bragg peaks at superlattice peak positions with h odd and main Bragg positions with h even can be recognized. At $T=358$ K, $\Delta T=5$ K above T_c, intense diffuse scattering around the superlattice positions and around the main Bragg peaks along the reciprocal a^* direction can be seen. At even higher temperature $T=374$ K, $\Delta T=21$ K the diffuse scattering is mainly centered around the main Bragg peak. This is the Huang scattering observed by Kanao *et al.*[11] (see inset of Fig. 1).

In the inset of Fig. 3 a typical spin-echo signal measured on the (1,2,0) superlattice peak at $T=335$ K is shown over a full period. To derive the spin-echo polarization $P_{\mathrm{NSE}}=(I_{\max}-I_{\min})/(I_{\max}+I_{\min})$ from these signals, a sine func-

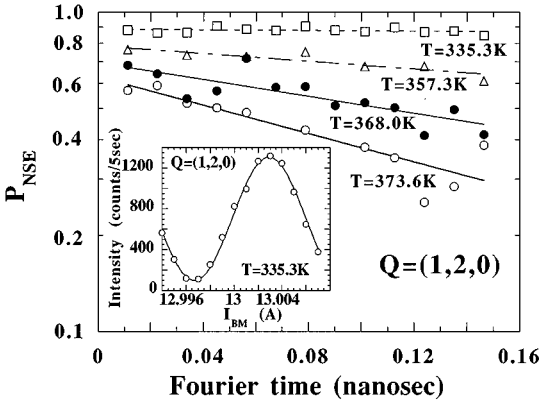

FIG. 3. Semilogarithmic plot of spin-echo polarization versus Fourier time at several temperatures. The lines indicate the results of exponential decay fits. Inset: A typical spin-echo signal over a full period measured on the superlattice peak (1,2,0). The solid line indicates the result of the sine-function fit, from which the spin-echo polarization is determined.

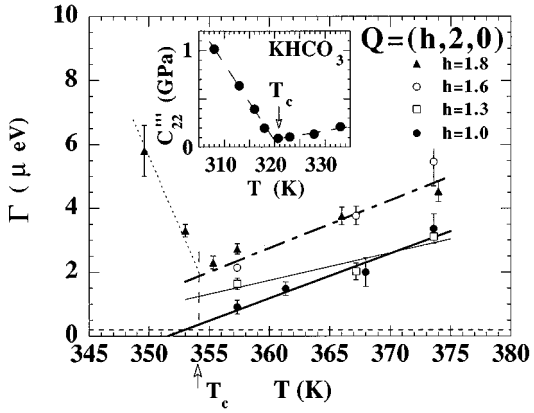

FIG. 4. Temperature dependence of a quasielastic linewidth at different $Q=(h,2,0)$. (●: $h=1.0$; □: $h=1.3$; ○: $h=1.6$; ▲: $h=1.8$.) The thick and thin solid lines are linear fits to the measured points at $h=1.0$ and 1.3, respectively. The dash-dotted line is a overall linear fit to the $h=1.6$ and 1.8 results above T_c. The dotted line is only a guide for the eye for $h=1.8$ below T_c. The dashed line indicates the spectral resolution of the instrument. The arrow indicates T_c as determined from the superlattice peak intensity (see inset of Fig. 2). Inset: Temperature dependence of the elastic constant in $KHCO_3$ (from Ref. 8). T_c as determined from the discontinuity of the critical scattering at (1.1,4,0) (Ref. 10) is indicated with the arrow.

tion is fitted to determine $I_{\max}$ and $I_{\min}$ as indicated by the solid line in the inset.

Figure 3 depicts the semilogarithmic plot of the spin-echo polarizations P_{NSE} versus the Fourier time at different temperatures on the superlattice peak position $Q=(1,2,0)$. It is clearly seen that the time correlations show simple exponential decays. The decay of the polarization measured on the superlattice peak at $T=335.3$ K$<T_c$ yields an instrumental energy resolution of ~ 0.2 μeV.

Figure 4 shows the T dependences of the relaxation coefficient Γ at various values of Q; $Q=(h,2,0)$ with $h=1.0$, 1.3, 1.6, and 1.8. One notices that the Γ value at $Q=(1,2,0)$ decreases linearly and extrapolates to the instrumental resolution of 0.2 μeV at $T\approx T_c$. The linear fit with $f(T)=\alpha(T-T_c)$ yields $T_c=352.8\pm0.9$ K in agreement with T_c determined from the superlattice peak intensity (see inset of Fig. 2). The coefficient α is determined to be $\alpha=(0.14\pm0.02)$ μeV/K.

As the h value is increased towards 2.0 (corresponding to the main Bragg position), the Γ values show an overall increase. At $Q=(1.6,2,0)$ and (1.8,2,0), where the diffuse scattering is mainly attributed to Huang scattering, the Γ values are approximately the same. Therefore, one may identify the relaxation coefficient in the Q region to be characterizing the dynamics of the strain field. The observed temperature variation clearly shows that the dynamical strain field also exhibits a slowing down towards the critical temperature. However, in contrast to Γ at $Q=(1,2,0)$, the relaxation constant remains finite even at $T=T_c$ and shows a rapid up turn as T is further lowered to $T<T_c$.

DISCUSSION

We find that the diffuse scattering in the vicinity of the superlattice position, $Q=(1,2,0)$, is due to the correlated fluctuation of the dimer reorientational mode. The observed results of $\Gamma(T)$ at $Q=(1,2,0)$ indicates complete critical slowing down phenomena as the temperature is lowered to T_c. On the other hand, Huang scattering which is associated with the strain field around each dimer does show incomplete slowing down. That is, although the relaxation constant decreases as T is lowered, it remains finite at $T=T_c$ and then increases rapidly as T is decreased further. It is interesting to compare these results with the elastic behavior of this material as observed by ultrasonic measurements.

Haussühl[8] carried out ultrasonic measurement to observe the temperature dependence of the elastic constants of $KHCO_3$. He points out that a particular elastic constant, C'''_{22}, exhibits remarkable softening as the temperature is lowered to T_c, which then hardens again as T is further lowered below T_c as depicted in the inset of Fig. 4. One immediately notices the similarity between the temperature dependence of $C'''_{22}(T)$ and $\Gamma(T)$ at Q values close to the main Bragg position. The linear fitting of both quantities with $f(T)=\alpha(T-T_c{}^*)$ commonly yields $T_c{}^*\sim T_c-10$ K. Recently, Kanao *et al.*[14] developed a theory to discuss the phase transition of $KH(D)CO_3$ by introducing the concept of pseudo-spin-phonon coupled system. Based on this theory, they show that in fact both C'''_{22} and Γ at $Q\sim(2,2,0)$ should give the temperature dependence given by $\alpha(T-T_c{}^*)$ in good agreement with the above experimental results.

Eckhold *et al.* carried out a neutron-scattering experiment on $KHCO_3$ in which they observed proton incoherent scattering which contain the information on the self-correlation of individual proton jump motions within a dimer. They concluded that the proton motion is strongly coupled to the reorientational motion of the dimer. Since the dynamical Huang scattering observed in the present experiment gives the relaxational motion of individual dimer, the observed dynamical behavior should also be associated with the dynamics of deuteron jump motion between the two deuteron self-trapped states. The characteristic time of 10^{-9} sec measured in the dynamical Huang scattering should be directly com-

pared with the average residence time of deuterons of 2.6×10^{-9} sec at 300 K as measured by NMR.[3]

Based on the static observation of the diffuse scattering, Kanao *et al.*[11] proposed that the interdimer interaction which causes the phase transition is mainly the indirect interaction mediated by the strain field. This interpretation seems plausible in a system where the dimers are strongly self-trapped, and relatively long residence time in one of the self-trapped states allows for the dimer to induce the strain field to mediate the interdimer interaction. The results of the present experiments give detailed information on the dynamical aspects of the phase transition mechanism for this concept.

To summarize, we reported the observation of the dynamical strain field scattering (dynamical Huang scattering) around the zone center above the order-disorder transition of $KDCO_3$ besides the critical slowing down at the zone boundary. Based on these observations the dynamical aspect of the phase transition in $KDCO_3$ has been clarified where the strain-mediated interactions between the $(DCO_3)_2$ dimers trigger the phase transition.

ACKNOWLEDGMENTS

We would like to thank Y. Kawamura, S. Watanabe, K. Nakajima, and M. Berneron for the technical assistance in setting up the thermal spin-echo option. The thermal neutron spin-echo project was supported in part by Yamada Science Foundation and by a Grant-in-Aid for Scientific Research from the Ministry of Education, Science, Sport, and Culture, Japan.

[1] A. Novak, P. Saumagne, and L.D.C. Bok, J. Chem. Phys. **60**, 1385 (1963).
[2] G. Lucazeau and A. Noval, J. Raman Spectrosc. **1**, 573 (1973).
[3] S. Benz, U. Haeberlen, and J. Tegenfeldt, J. Magn. Reson. **66**, 125 (1986).
[4] J.O. Thomas, R. Tellgren, and I. Olovsson, Acta Crystallogr. **B30**, 1155 (1974).
[5] F. Fillaux, J. Tomkinson, and J. Penfold, Chem. Phys. **124**, 425 (1988).
[6] F. Fillaux, Chem. Phys. **74**, 405 (1983).
[7] A. Stöckli, B.H. Meier, R. Kreis, R. Meyer, and R.R. Ernst, J. Chem. Phys. **93**, 1502 (1990).
[8] S. Haussühl, Solid State Commun. **57**, 643 (1986).
[9] S. Kashida and K. Yamamoto, J. Solid State Chem. **86**, 180 (1990).
[10] G. Eckold, H. Grimm, and M. Stein-Arsic, Physica B **180&181**, 336 (1992).
[11] L. Kanao, S. Nohdo, N. Horiuchi, S. Kashida, K. Kakurai, and Y. Yamada, J. Phys. Soc. Jpn. **64**, 2286 (1995).
[12] C.M.E. Zeyen, K. Kakurai, M. Nishi, K. Nakajima, T. Sakaguchi, Y. Kawamura, S. Watanabe, M. Berneron, K. Sasaki, and Y. Endoh (unpublished).
[13] O. Schärpf, in *Neutron Spin Echo*, edited by F. Mezei (Springer-Verlag, Berlin, 1980), p. 27.
[14] L. Kanao *et al.* (unpublished).